Response of the $^1P^o$ resonance near $n=3$ in the H^- continuum to external electric fields

Stanley Cohen
Drexel University, Philadelphia, Pennsylvania 19104

H. C. Bryant, C. J. Harvey, and J. E. Stewart
University of New Mexico, Albuquerque, New Mexico 81731

K. B. Butterfield, D. A. Clark, J. B. Donahue, and D. W. MacArthur
Los Alamos National Laboratory, Los Alamos, New Mexico 87545

G. Comtet
Universite Paris-Sud, 91400 Orsay, France

W. W. Smith
University of Connecticut, Storrs, Connecticut 06268
(Received 22 June 1987)

The response to external electric fields of the $^1P^o$ resonance "dip" in the H^- photodetachment continuum cross section below the $n=3$ hydrogenic excitation threshold is investigated. Using the relativistic ($\beta=0.806$) 650-MeV H^- beam at the Clinton P. Anderson Meson Physics Facility (LAMPF) in Los Alamos, the fourth harmonic (266 nm) of a Nd:YAG laser (where YAG denotes yttrium aluminum garnet) is Doppler shifted to provide a continuously tunable photon beam in the rest frame of the ions. The magnetic field from pulsed Helmholtz coils, surrounding the photon-H^- interaction point provides a Lorentz-transformed barycentric electric field. As the magnitude of the external field is increased, there is no observed shift in the photon energy to excite the resonance E_o, 12.650±0.001 eV, until quenching occurs at a field strength of 2.36 MV/cm. The effective strength of the resonant state is consistent with a linear decrease with increasing field. The line shape index q is constant within statistical uncertainty, until the resonance disappears. There is evidence that the width of the resonance remains constant at fields below 1.25 MV/cm. It then broadens at higher fields before the resonance quenches.

INTRODUCTION

Although the negative hydrogen ion (H^-) is a simple atomic system, describing its structure even with nonrelativistic quantum mechanics is not a trivial exercise. Experimental data from this three-body Coulomb system are viewed with great interest since H^- can be used as a test bed for checking the validity of theoretical models in atomic and molecular physics. Observations of its ionization threshold behavior and resonant structure have provided stimuli for theoretical investigations of short-range electron correlation effects and bound states in the continuum. Risley[1,2] provides a comprehensive historic review of experimental investigations of the H^- ion. Current theoretical work especially relevant to this paper includes, for example, that by Lin,[3–5] Ho,[6] Greene,[7,8] and Callaway.[9,10]

The H^- ion has only one state whose energy is below the first ionization level of the system.[11,12] This is, strictly speaking, the only bound state of the system.

Most excited states (resonances) of the ion are doubly excited and autoionizing, that is, the H^0 core of the system is excited and an electron is subsequently spontaneously ejected leaving atomic hydrogen. A putative $^3P^e$ (triplet P, even parity) state is the only doubly excited state that is not autoionizing.[13] Resonances can be studied through electron-hydrogen scattering,[14] or by observing the photodetachment spectrum of H^-.

High-resolution studies of the H^- ion are performed at the 800-MeV proton linear accelerator at the Clinton P. Anderson Meson Physics Facility (LAMPF) at Los Alamos. Experimental details of this work will be discussed later.

Experiments at LAMPF have identified the Feshbach and shape resonances near the hydrogenic $n=2$ threshold,[15] documented the response of these resonances to moderate and strong external electric fields,[16–18] and identified recursions of the $^1P^0$ closed-channel resonances below $n=3$.[19] Reviews of these experiments have been published by Bryant,[20] Bryant *et al.*,[21] and Smith *et al.*[22] This present work reports observations of the response of the resonant states near the $n=3$ hydrogenic excitation threshold to external electric fields of 0–2.5 MV/cm.

PREDICTIONS OF RESONANCES NEAR $n=3$

Gailitis and Damburg[23,24] have proposed that the resonances that lie below hydrogenic thresholds above $n=2$ exponentially approach the threshold in the fol-

lowing way:

$$\frac{E_t-E_n}{E_t-E_{n+1}}=\frac{\Gamma_n}{\Gamma_{n+1}}=\exp(2\pi/(\mathrm{Im}\sqrt{|a+1/4|}))\ , \qquad (1)$$

where (E_t-E_n) is the distance in energy of the nth resonance from the threshold. Here, Γ_n is the energy width of the nth state, and a is related to $l(l+1)+\alpha$, constructed from coefficients of centrifugal and dipole terms in close-coupling equations between channels opening under the $n=3$ threshold. The coefficient a is the strength of the long-range potential $V(r)\rightarrow -a/2r^2$. The threshold behavior differs depending on the sign of $a-\frac{1}{4}$. For $a>\frac{1}{4}$, in a.u., an infinite number of bound states below threshold are predicted; the number will be finite if $a\leq\frac{1}{4}$.[25-27] Gailitis[28] tabulated the locations of the H^- resonances converging to the hydrogenic $n=3$ threshold. Herrick,[29] Kellman and Herrick,[30,31] Herrick *et al.*,[32] Gailitis,[33] and Read[34] have searched for symmetries that could predict the positions of resonant states. Herrick *et al.*[32] have used a group-theoretical approach to classify resonant states.

A number of techniques have been used to calculate energies of the H^- bound states. Ho and Callaway[35] use a method of complex-coordinate rotation. Ho[36] used this method to calculate the locations of the resonances observed by Hamm *et al.*[19] Agreement for both the location and width of the resonances was quite good, as can be seen in Table I. The complex coordinate method is reviewed by Ho.[37]

Greene[25] has been able to confirm the experimental observations of Hamm *et al.*[19] using a combined hyperspherical coordinate and semiempirical quantum-defect theoretical (QDT) approach.

Observations of states near $n=3$ were reported earlier by McGowan, Williams, and Curley,[38] Williams,[39] and others in the context of e^--H^0 scattering. The experimental technique used by Hamm *et al.*,[19] which is essentially the same as is used here, has an energy resolution of 6 meV. To date there has been little theoretical exploration of the effects of an external electric field on the bound states between $n=2$ and 3.

The results presented here are the continuation of the investigations of the other observations of the resonant structure in the H^- photodetachment spectrum near $n=3$ reported by Hamm *et al.*[19]

The experimental apparatus used for this present investigation is that described by Butterfield.[18] A brief description of the experimental method follows.

DOPPLER TUNING

The key to our ability to determine accurately the energy of the incident photon is the availability at LAMPF of the high-quality, relativistic H^- ion beam (i.e., small angular divergence, narrow momentum spread, and with particle velocities near the speed of light). With these ultrafast ions, the relativistic Doppler shift can be exploited to produce a tunable photon source in the ion's rest frame.

For a given photon laboratory energy, E_{lab}, the photon's energy in the H^- rest frame is given by

$$E=E_{\mathrm{lab}}\gamma(1+\beta\cos\alpha)\ . \qquad (2)$$

Here $\beta=v/c$, where v is the speed of the ion in the laboratory frame, c is the speed of light in a vacuum, $\gamma=(1-\beta^2)^{-1/2}$, and α is the intersection angle of the photon and ion beams, such that $\alpha=0$ is a head-on collision, as shown in Fig. 1. For an ion beam with a kinetic energy of 650 MeV, a center-of-mass photon-energy range of 1.523–14.25 eV can be obtained using the 4.6595-eV photon, the fourth harmonic derived from a fixed-frequency Nd:YAG laser (where YAG denotes yttrium aluminum garnet).

Our knowledge of the center-of-mass photon energy is

TABLE I. Comparison of various predicted parameters of the $^1P^o$ dip of H^- below $n=3$ and the experimental results. The resonance position is shown first, in the author's units then common units of electron volts (eV) to allow comparison. The Ry_∞ 13.605 84(36) eV, electron affinity for H^- of 0.7542 eV, and the conversion factor of 1 a.u. = 27.211 608 eV are used to deduce the resonance energy position, E_0 as measured from the H^- ground state.

Reference	Authors	Method	Resonance position Theoretical		(eV)	Width (eV)	Line shape index
51	Burke, Ormonde, Wittaker	6-state close coupling	0.8758	Ry	12.670	0.0383	
52	Oberoi	Feshbach formalism	0.12491	Ry	12.652		
53	Chung	Feshbach formalism	0.0625	a.u.	12.654		
54	Herrick, Sinanoglu	Group theoretical prediction	11.923	eV	12.677		
55	Morgan, McDowell, Callaway	12-state close coupling	0.87495	Ry	12.6586	0.0462	
56	Ho	Complex rotation	0.12535(1)	Ry	12.6585	0.0337(2)	
57	Lipsky, Anania, Conneely	Feshbach formalism	0.062342	a.u.	12.6494		
58	Callaway	18-state close coupling	0.874568	Ry	12.6534	0.0325	
59	Greene	Hyperspherical coordinates	−173	mV	12.669		
59	Ho	Complex rotation	0.12542	Ry	12.6594	0.0318	
			Experimental				
38	McGowan, Williams, Curely	e impact	11.89(2)	eV	12.64(2)		
39	Williams	e impact	11.85(6)	eV	12.60(6)		
19	Hamm *et al.*	Photodetachment			12.646(4)	0.0275(8)	−0.81(2)
	Present Experiment	Photodetachment			12.650(7)	0.0392(2)	−0.7(4)

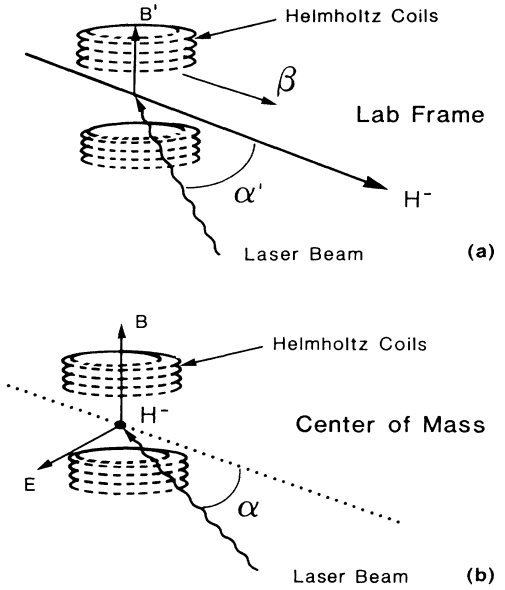

FIG. 1. Colliding H^- ion and photon beams. (a) Laboratory frame, (b) center-of-mass frame.

based upon how well we can determine the intersection angle, α, of the colliding beams and the velocity, β, of the ion beam. The photon-energy resolution of the experiment has two principal components, the energy spread due to the angular uncertainty,

$$\frac{\delta E}{E}=\beta\frac{\sin\alpha}{1+\beta\cos\alpha}\delta\alpha \tag{3}$$

and the energy spread due to the ion-beam velocity,

$$\frac{\delta E}{E}=\frac{\delta p(\beta^2+\beta\cos\alpha)}{p(1+\beta\cos\alpha)} . \tag{4}$$

Note that if $\alpha=\cos^{-1}(-\beta)$ in Eq. (4), the energy uncertainty due to the spread in the H^- beam momentum vanishes. This angle is called the "relativistic Doppler-free angle." For a 650-MeV ion beam this angle is approximately 144°.

CENTER-OF-MASS ELECTRIC AND MAGNETIC FIELDS

Motional barycentric electric fields in the megavolt per centimeter (MV/cm) range can be attained by further exploitation of special relativity. For a laboratory magnetic field, B', perpendicular to the velocity of ion beam, v, an electric field orthogonal to both B' and v will exist with a field strength of

$$F=\gamma\beta cB' . \tag{5}$$

The center-of-mass magnetic field is

$$B=\gamma B' . \tag{6}$$

An ion beam with a β of 0.8062 ($E_{\rm kin}=650$ MeV) will see a transverse electric field of about 1 MV/cm and a magnetic field of 5 kG from a laboratory magnetic field of a modest 3 kG.

The analysis of data from the current experiment will ignore the influence of motional magnetic field on the ions. The ratio of the coupling energies is estimated by Bryant *et al.*[21] to be

$$E_F/E_B=2\beta/\alpha_0 , \tag{7}$$

where E_F is the coupling of the ion to the electric field and E_B is the coupling to the magnetic field. α_0 is the fine-structure constant. The ratio is about 200.

CALCULATING THE CROSS SECTION

The photodetachment cross section can be calculated using the relation[22]

$$\sigma=\frac{GR\beta\sin\alpha}{IJ(1+\beta\cos\alpha)} , \tag{8}$$

where R is the rate of photodetachment fragment production, I and J are the photon- and ion-number currents. G is a geometric factor that represents the spatial and temporal overlap of the crossed beams. For two continuous, perfectly overlapping cylinders of the same radius r,

$$G=(3\pi^2 rc)/16 . \tag{9}$$

This factor currently can only be estimated for the present experimental configuration and the cross sections presented here are therefore only relative.

Enveloping the photon-H^- interaction region, as shown in Fig. 1, are a pair of Helmholtz coils (the "Stark magnet") that provide the laboratory magnetic field perpendicular to the ion beam and, hence, crossed magnetic and electric fields in the center of mass. A pulse of current is sent through the coils that is timed to coincide with the photon pulse reaching the H^- interaction region. The timing of the current pulse is adjusted so that the magnetic field is constant before the beam pulses arrive and remains constant for a period much longer than the photon-ion interaction. (The magnet-pulse duration is 1.8 μsec and the laser pulse duration is 10 nsec.) Details of the magnet development and operation are presented by Butterfield[18] and Krausse and Butterfield.[40]

Any fragments generated in the photodetachment will be either electrically neutral or positively charged. A downstream magnet separates H^0 and H^+ from the

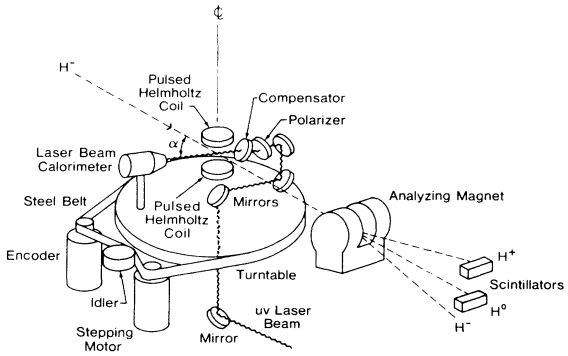

FIG. 2. Scattering chamber with associated optics and detectors.

negative-ion beam. The deflected particles are detected by a scintillation counter. The particle trajectories are shown in Fig. 2.

The YAG laser, mirrors, and scattering chamber are mounted on an optical bench. The output of the laser harmonic generator is directed by the mirrors through a window at the bottom center of the evacuated scattering chamber and up to the mirrors of a turntable which is driven by a steel belt connected to a stepping motor. The angular position of the turntable, α, is digitized by an optical encoder, as shown in Fig. 2. The encoding scheme used here has an effective resolution of 18 bits per 2π radians, or about 31 mrad.

Laser-beam intensity is sampled by vacuum photodiodes positioned on the optical table to pick up scattered light from the mirrors in the beam line. A value for laser intensity at the interaction point is provided by a calorimeter inside of the laser-beam catcher on the turntable in the scattering chamber.

DATA ACQUISITION

We define a run as the sequential measurement of cross sections at equally spaced preselected laser angle increments, 100 encoder steps. Data acquisition, turntable motor control, and laser and magnet-pulse timing are controlled by a minicomputer and other associated electronics. Just as the currents in the beam line magnets have to be adjusted to assure spatial overlap of the two beams, the control electronics must be set to assure the temporal overlap of the laser pulse, a 0.25-ns-long H^- pulse (micropulse) from the LAMPF linear accelerator, and the Stark magnetic pulse. A photodetachment spectrum is generated by calculating the cross section at each laser-ion beam angle and corresponding photon energy.

As noted above, cross sections measured are relative, because of spatial and temporal uncertainties. The problem of synchronizing the arrival of the photons with a short burst of ions is exacerbated by the 5-ns output jitter of the laser. Typically the timing of the laser trigger is arranged so that a photon pulse occurs in the center of a macropulse (a 500-μsec train of micropulses).

DATA ANALYSIS

The experimental energy resolution [Eqs. (3) and (4)] can be determined from the observed energy width of a narrow feature in the H^- spectrum considered to be a δ function for our purposes. For this current work the measured width of the $^1P^o$ Feshbach resonance just below the hydrogenic $n=2$ level was used to determine the energy resolution for this experiment.

Fitting of the experimental data was done in three phases.

(1) Calibration of the data to a feature in the H^- spectrum whose energy is known.

(2) Normalization of the measured relative cross sections to a consistent value.

(3) Fitting the normalized spectra to an assumed functional form.

The $^1P^o$ Feshbach resonance below $n=2$ was used as an energy benchmark. Its location has been well established in previous experiments,[41] and the feature is easily accessible for measurement. Its energy can be measured with the same experimental configuration as the nearby resonances of interest in this work near the hydrogenic $n=3$ level. With an ion-beam kinetic energy of 650 MeV, the Feshbach resonance is located about 10° away from the $n=3$ threshold angle. Calibration runs near $n=2$ are interspersed with the $n=3$ runs, assuring similar observational conditions. The splitting of the Feshbach resonance with increasing external electric fields[19] provides a cross check for the Stark-magnetic field values.

Since α for the Feshbach resonance should be the same on both sides of the ion beam, the location of this resonance is also used to determine the encoder reading for which $\alpha=0$, a purely geometric exercise. Once the location is known, the value of β can be calibrated to place the resonance at the correct absolute angle location [Eq. (2)].

The values we obtain for the photon-H^- cross section are reliable up to a geometric factor G [Eq. (9)]. During one run, lasting about one hour, conditions are usually constant. The relative photodetachment cross sections measured during a run will be internally consistent. Over the course of a day or two, beam intensities and positions of both the ion and photon beams often change sufficiently to yield different relative cross sections at the same energy. We chose to normalize all spectra so that the continuum cross section far from the resonance has the same average value. The weighted average of the five lowest energy points of a scan with no external electric field applied is used to compute a normalization factor for both field and no-field data.

The observed cross sections near $n=3$ have been fitted to a Fano line shape introduced by Fano line shape introduced by Fano and Cooper[42] and used by Hamm *et al.*[19] in their analysis of the field-free shape of this $^1P^o$ resonance. The functional form that arises from the coherent addition of the amplitude of a Breit-Wigner[43] resonance and constant continuum is

$$\sigma(\varepsilon)=\sigma_a\frac{(q+\varepsilon)^2}{1+\varepsilon^2}+\sigma_b\ , \tag{10}$$

where $\varepsilon=(E-E_0)/(\Gamma/2)$, with Γ being the full width at half maximum (FWHM) of the resonance, E_0 its center, σ_a the resonant cross section, σ_b the nonresonant cross section, and q the line profile index. For each fitting calculation E_0, Γ, q, σ_a and σ_b were free parameters. Both the parameter values and standard deviations were calculated in Table II. The fitting algorithm used is a rigorous least-squares adjustment based upon a method outlined by Wentworth[44] and Demming.[45]

As a check on the reliability of the fitting method, simulated data were generated using a known parent Fano function. These data were analyzed and the fitted parameters were compared to those of the parent. The central values of the fitted data were in good agreement with the chosen functional values.[46]

TABLE II. Fitted parameters of energy scans (see text).

Run E (MV/cm)	E_0 std dev	Γ	q	σ_a	σ_b
no-field average	12.6500	0.0390	−0.7169	4.1054	4.4770
0.0	0.0010	0.0020	0.0372	0.2000	0.1350
1 [Fig. 4(c)]	12.6502	0.0581	−0.5807	2.7747	6.5317
1.18	0.0052	0.0081	0.1211	0.4138	0.2884
2	12.6203	0.0568	−3.0960	0.1907	9.3402
2.36	0.0100	0.0221	1.5006	0.1880	0.1680
3 [Fig. 4(d)]	12.6206	0.1118	−1.3369	0.5060	7.8701
2.36	0.02666	0.0377	0.8607	0.8167	0.2100
4 [Fig. 4(b)]	12.6463	0.0357	−0.9809	2.3206	4.9730
0.69	0.0032	0.0059	0.1782	0.5102	0.3074
5	12.6457	0.0323	−0.7842	4.6676	5.9586
0.24	0.0023	0.0054	0.1032	0.6601	0.5694
6	12.5887	0.0905	−1.9103	0.4724	8.6113
2.36	0.0284	0.0416	0.9750	0.7862	0.3357
7	12.6328	0.0444	−0.9231	3.5910	5.0871
0.79	0.0041	0.0082	0.1410	0.6480	0.5058
8	12.6365	0.0191	−0.6505	3.2362	5.7002
1.18	0.0046	0.0095	0.2428	1.2949	1.2365
9	12.6455	0.0854	−0.4620	2.2562	6.0556
1.97	0.0162	0.0480	0.2116	0.7020	0.5770

RESULTS

The results of the analysis for scans in the energy region of the $^1P^o$ resonance are presented here. In order to correct for the energy resolution of the experimental apparatus, the resolution, determined from Feshbach resonance measurements, was subtracted in quadrature from the fitted value of the width (Γ). The results of our energy-resolution study indicated that other fitted Fano parameters were not significantly sensitive to resolutions of 20 meV or less; no corrections to these parameters were calculated.

To evaluate the response of the resonance to an external electric field, the effective strength (S_{eff}) of the resonance is also computed,[47]

$$S_{\text{eff}}=[\sigma_a/(\sigma_a+\sigma_b)]^2(q^2+1)\ . \tag{11}$$

The effective strength of the resonance near $n=3$ with zero field is 0.34, compared to the value of the shape resonance of about 35.[19] This two-orders-of-magnitude difference in effective strength makes the $n=3$ resonance much more difficult to measure.

THE RESONANCE WITH NO EXTERNAL FIELD

It is instructive to examine first the spectra obtained with no external electric field. These can be compared to earlier experimental results.[19] The scans in this series [Fig. 3(c)] extend through 12.83 eV, the measured location of the second recursion of the $^1P^o$ resonance.

Table III compares the corrected no-field weighted average of this work with the results of Hamm *et al.*[19] There is a disagreement in the width (Γ) obtained in the two experiments. The researchers in the former experiment did not have access to as well defined an energy scale as does the present experiment. Cross-section data from different runs were arbitrarily shifted in energy so that data points visually lined up; this could have contributed to the significant difference in the value of the width parameter since it is the most sensitive to small changes in energy.

EFFECTS OF THE EXTERNAL FIELD

Figure 4 represents measurements taken within a few minutes of each other, and shows the progression of the shape of the $^1P^o$ resonant structure as the applied external electric field is increased. An illustration of the complete quenching of the $^1P^o$ resonance in a strong (2.36 Mv/cm) external electric field is shown in Fig. 4(d). Table II presents the fitted parameters of all of the scans taken in the energy region of the $^1P^o$ resonance with a different external electric field.

The spectra in Fig. 4 provide a qualitative feel for the effect of the increasing electric field on the resonance. By examining the effect of the field on each fitted Fano parameter, more quantitative knowledge about the behavior of the resonance can be gained. Resonance quenching is illustrated in Fig. 5(c), which shows the effective strength as a function of external field. The data have been fitted to a straight line. The electric field intercept of the linear fit is 2.6 MV/cm, which is probably an overestimate for the field required for full quenching. Fits using the highest field data cannot be relied upon to give consistent results.

A study of the width (Γ) data in Fig. 5(b) reveals what appears to be a plateau in value of Γ, below the electric field values of 1 MV/cm. A similar tendency for the resonance to narrow before broadening has also been identified in the behavior of the shape resonance just above $n=2$.[48]

The last set of plots, Fig. 6, presents a graphical sum-

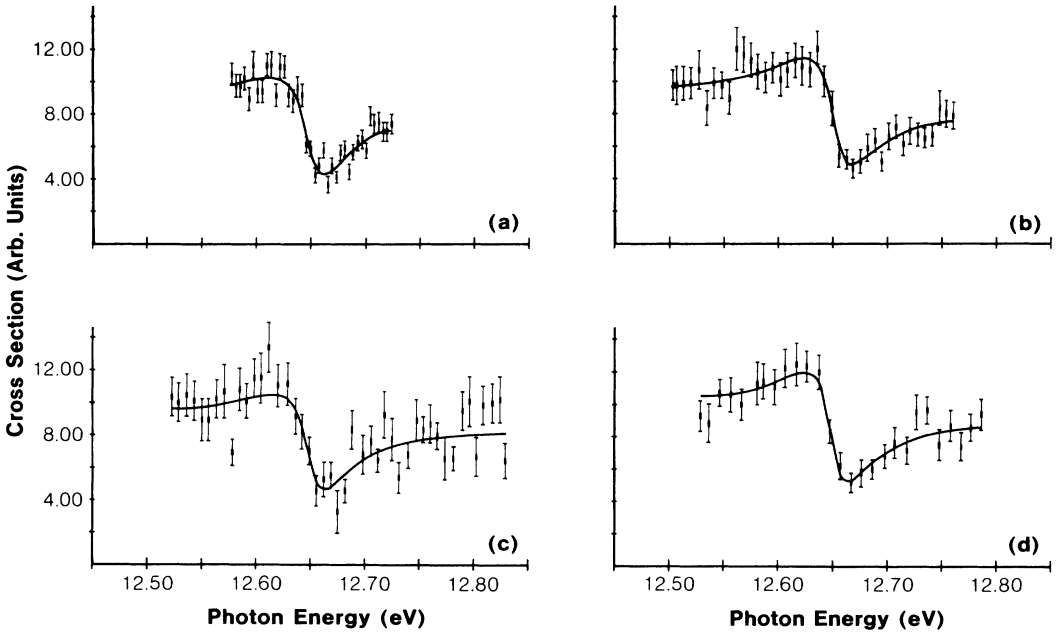

FIG. 3. Four sample resonance spectra in the absence of an external electric field.

mary of the parameters obtained by fitting a selection of no-field scans. The ordinate for each of the charts is an arbitrary run number, chosen so that the data points are evenly spaced vertically. Each datum is displayed as a central value plus a horizontal "error bar" indicating the standard deviation for the fit. A Gaussian probability function for each parameter has been calculated. The area of the Gaussian for each fitted parameter is $1/\sigma$. Using a weight of $1/\sigma$ instead of $1/\sigma^2$, as one does to compute a weighted average, tends to emphasize systematic errors over statistical ones.[49] For totally consistent experimental data the resulting plot, an "ideogram," should be a symmetric curve with a single peak. An ideogram is superimposed on each graph in Fig. 6. The weighted averages of these parameters are displayed as a vertical line plotted at the appropriate location on each chart in Fig. 6.

CONCLUSIONS

This work reports the first systematic study of the response of the $^1P^o$ resonance below $N=3$ to external electric fields. Measurement of the resonance spectrum near the $N=3$ threshold presents a greater experimental challenge than the region near $n=2$, since the effective strength of the $n=2$ shape resonances (Ref. 35) is approximately 100 times that of the $^1P^o$ resonance at $N=3$ (0.34).

The present investigation clearly shows the quenching of the resonance as a function of external field strength. Substructure is not evident which might indicate the mixing of nearby states, i.e., S and D states, with the P state. The resistance to quenching in external fields less than 1.5 MV/cm supports the + classification of the observed state. The + state, shape resonance, just

TABLE III. Comparison of corrected fitted parameters for a fit (the weighted average of all no field scans) to Hamm *et al.* (Ref. 19).

Parameter	Hamm *et al.*	This experiment
E_0	12.646±0.004	12.650±0.001
Γ	0.0275±0.0008	0.0390±0.002
q	−0.81±0.02	−0.716±0.37
σ_a		4.11±0.200
σ_b		4.47±0.135
Effective strength	0.32±0.02	0.34±0.02

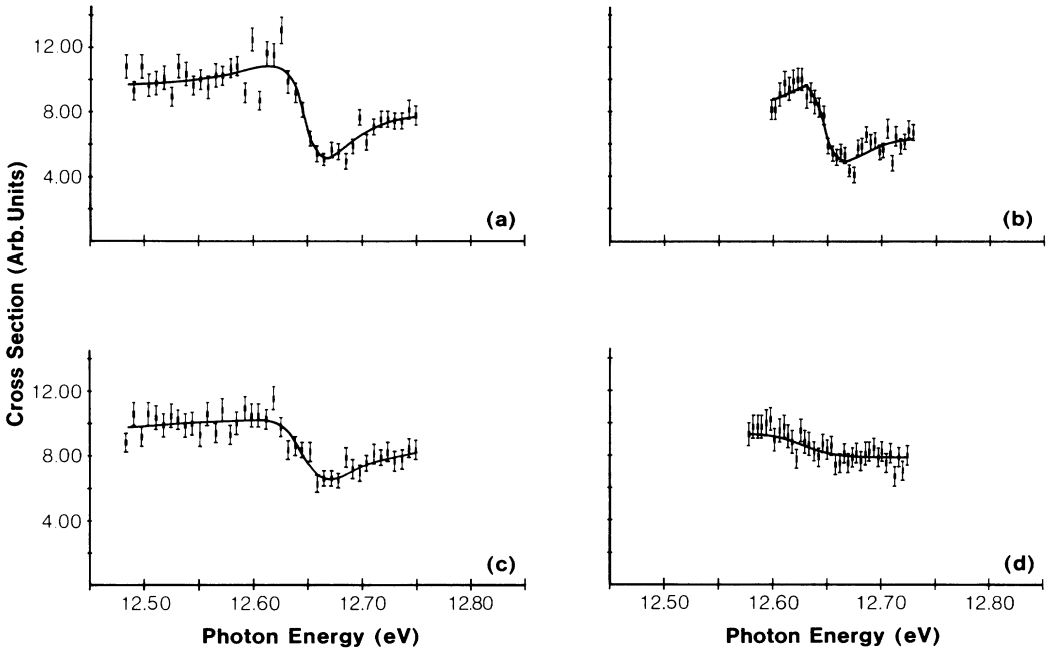

FIG. 4. Evolution of the shape of the $^1P^o$ resonance in increasing external electric fields. The fields are (a) no field, (b) 0.69 MV/cm, (c) 1.18 MV/cm, (d) 2.36 MV/cm.

above $n=2$, exhibits the same durability in strong electric fields.

Lin[5] points out that as the external field increases, the potential well gets narrower. At sufficiently large fields the well can no longer support a bound state. As increasing electric fields narrows the potential barrier, the lifetime of the resonant state decreases through quantum-mechanical tunneling.

One would expect a downward shift of E_0, tracking the downward quadratic Stark shift of the $n=3$ hydrogenic threshold itself as greater values of electric field are applied.[50] The statistical uncertainty exhibited in

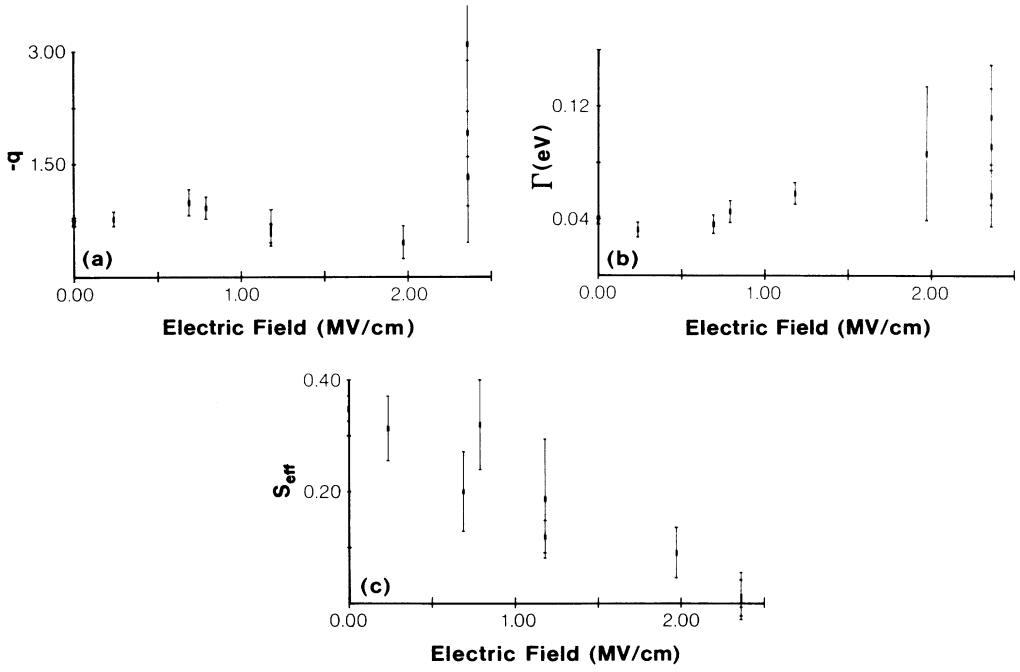

FIG. 5. Summary of fitted parameters as a function of external electric field. (a) q, (b) Γ. Note the "plateau region" in the 0.1–0.8-MV/cm range of external field. (c) Effective strength. See Eq. (11) in the text.

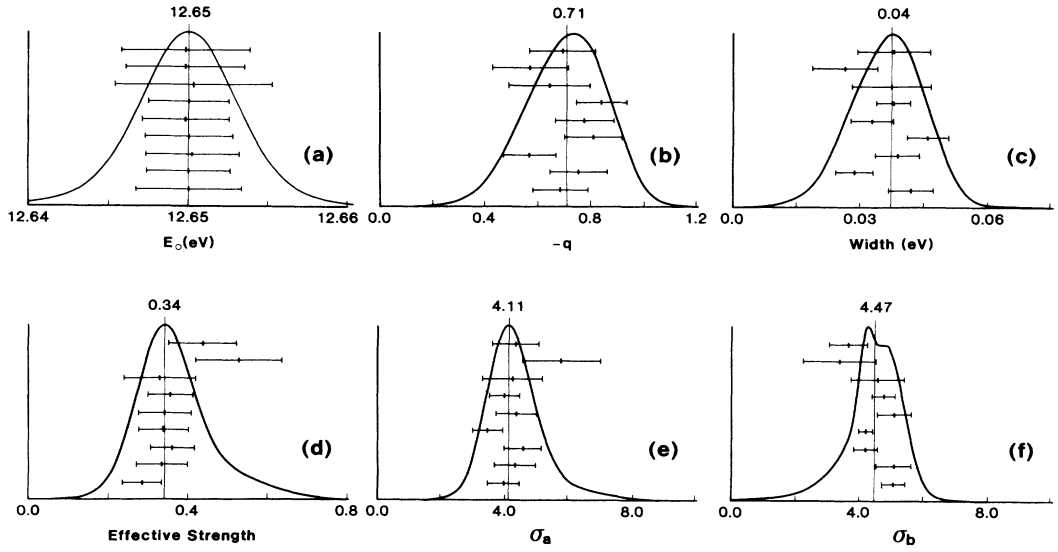

FIG. 6. Ideograms of no-field parameters. (a) E_0, (b) $-q$, (c) Γ, (d) effective strength, (e) σ_a, and (f) σ_b.

data sets such as Fig. 6(c) would tend to obscure any detectable shift in E_0.

A lack of noticeable change in E_0 could be due to the Stark shift and potential narrowing working against each other. One would expect E_0 to *rise* as the potential well narrows, thus canceling the downward Stark shift.

There is a possibility that the line shape narrows at moderate fields. A detailed study at moderate fields would provide more substantial evidence to confirm or deny the existence of this narrowing. Understanding the mechanism of the narrowing, possibly due to coherent mixing with narrower resonances, could also shed light on the mechanism of quenching itself. Measurements performed with light of a known polarization were of poor quality and are not shown here.

There is lack of agreement of the fitted width (Γ) of the present no-field data with that of the only previous measurements.[21] Energy calibration and the validity of fitting routines used in this investigation have been carefully verified. The disagreement will need to be resolved by gathering further experimental data in the future.

Hamm *et al.*[19] reported a second recursion of the $^1P^o$ resonance at about 12.83 eV that is not evident in this study. Its existence may be masked in this work by the high statistical error of the scans that covered this region.

In summary, the findings of this investigation are as follows.

(1) The width of the $n=3$ resonance, in external electric fields below 1 MV/cm, remains relatively constant, before broadening at higher field values. A similar phenomenon has been observed in the + symmetry shape resonance just above $n=2$.

(2) There is no shift of E_0 with increasing external field strengths.

(3) The $^1P^o$ resonance quenches completely at a field strength of greater than 2.36 MV/cm.

(4) Within our present experimental resolution the location of the $^1P^o$ resonance has been reconfirmed. Its quenching in a strong external electric field has been documented for the first time. Its behavior in moderate fields is demonstrated.

ACKNOWLEDGMENTS

Dr. Peter Gram, Jim Hontas, George Krausse, and John Gomez contributed in a significant way to the success of this experiment. This work was done under the auspices of the U.S. D.O.E., Division of Chemical Sciences, Office of Basic Energy Sciences, Office of Energy Research, in part under contract DE-AS04-77ERO-3998.

[1]J. S. Risley, in *Proceedings of the 4th International Conference on Atomic Physics* (Plenum, New York, 1975).
[2]J. S. Risley, in *Proceedings of the 6th International Conference on Atomic Physic* (Plenum, New York, 1978).
[3]C. D. Lin, Phys. Rev. A **14**, 130 (1979).
[4]C. D. Lin, Phys. Rev. A **23**, 1585 (1981).
[5]C. D. Lin, Phys. Rev. Lett. **51**, 1348 (1983).
[6]Y. K. Ho, **77A**, 147 (1980).
[7]C. H. Greene, J. Phys. B **13**, L39 (1980).
[8]C. H. Greene, Phys. Rev. A **20**, 656 (1979).
[9]J. Callaway, Phys. Lett. A **75**, 43 (1979)
[10]J. Callaway, Phys. Lett. A **68a**, 315 (1978).
[11]R. N. Hill, Phys. Rev. Lett. **38**, 643 (1977); J. Math. Phys. **18**, 2316 (1977).
[12]D. R. Beck and C. A. Nicolaides, Chem. Phys. Lett. **59**, 525 (1978).

[13]G. W. F. Drake, Phys. Rev. Lett. **24**, 126 (1970).
[14]G. J. Schultz, Rev. Mod. Phys. **45**, 378 (1973); Phys. Rev. Lett. **13**, 583 (1964); Phys. Rev. **136**, A650 (1964).
[15]H. C. Bryant, B. D. Dieterlie, J. B. Donahue, H. Sharifian, H. Tootoonchi, P. A. M. Gram, D. M. Wolfe, and M. Yates, Phys. Rev. Lett. **38**, 228 (1977).
[16]P. A. M. Gram, J. C. Pratt, M. A. Yates-Williams, H. C. Bryant, J. B. Donahue, H. Sharifian, and H. Tootoonchi, Phys. Rev. Lett. **40**, 107 (1978).
[17]H. C. Bryant, D. A. Clark, J. B. Donahue, K. B. Butterfield C. A. Frost, H. Sharifian, H. Tootoonchi, P. A. M. Gram, M. E. Hamm, R. W. Hamm, J. C. Pratt, M. A. Yates, and W. W. Smith, Phys. Rev. A **27**, 2889 (1983).
[18]K. B. Butterfield, Ph.D. Dissertation, University of New Mexico, LANL Report No. LA-10149-T, 1984 (unpublished).
[19]M. E. Hamm, R. W. Hamm, J. Donahue, P. A. M. Gram, J. C. Pratt, M. A. Yates, R. D. Bolton, D. A. Clark, H. C. Bryant, C. A. Frost, and W. W. Smith, Phys. Rev. Lett. **43**, 1715 (1979).
[20]H. C. Bryant, in *Proceedings of the Eleventh International Conference on the Physics of Electronic and Atomic Collisions, Kyoto, 1979,* edited by K. Takayanga and N. Oda (The Society for Atomic Collision Research, Kyoto, 1979).
[21]H. C. Bryant, K. B. Butterfield, D. A. Clark, C. A. Frost, J. B. Donahue, P. A. M. Gram. M. E. Hamm, R. W. Hamm, and W. W. Smith, in *Atomic Physics 7,* edited by D. Kleppner and F. M. Pipkin (Plenum, New York, 1981).
[22]W. W. Smith, C. Harvey, J. E. Stewart, H. C. Bryant, K. B. Butterfield, D. A. Clark, J. B. Donahue, P. A. M. Gram, D. W. MacArthur, G. Comtet and T. Bergeman, in *Atomic Excitation and Recombination in External Fields,* edited by M. H. Nayfeh and C. W. Clark (Harwood Academic, New York, 1985).
[23]M. Gailitis and R. Damburg Zh. Eksp. Teor. Fiz. **44**, 1644 (1963) [Sov. Phys.—JETP **17**, 1107 (1963)].
[24]M. Gailitis and R. Damburg, Proc. Phys. Soc. London **82**, 192 (1963).
[25]C. H. Greene and A. R. P. Rau, Phys. Rev. A **32**, 1352 (1985).
[26]A. Temkin, Phys. Rev. Lett. **49**, 365 (1982).
[27]A. Temkin, Phys. Rev. A **30**, 2737 (1984).
[28]M. Gailitis, J. Phys. B **13**, L479 (1980).
[29]D. R. Herrick, J. Math. Phys. **16**, 1047 (1975).
[30]D. R. Herrick and M. E. Kellman, Phys. Rev. A **21**, 418 (1980).
[31]M. E. Kellman and D. R. Herrick, Phys. Rev. A **22**, 1536 (1980).
[32]D. R. Herrick, M. E. Kellman, and D. R. Poliak, Phys. Rev. A **22**, 1517 (1980).
[33]M. Gailitis, in Proceedings of the 6th International Conference on Atomic Physics, 1978 (unpublished).
[34]F. H. Read, Aust. J. Phys. **35**, 475 (1982).
[35]Y. K. Ho and J. Callaway, Phys. Rev. A **27**, 1887 (1983).
[36]Y. K. Ho, Phys. Rep. **99**, 1 (1983).
[37]Y. K. Ho, J. Phys. B **10**, L373 (1977).
[38]J. W. McGowan, J. F. Williams, and E. K. Curley, Phys. Rev. **180**, 132 (1969).
[39]J. F. Williams, J. Phys. B **9**, 1519 (1976).
[40]G. J. Krausse and K. B. Butterfield in Proceedings of the IEEE 16th Power Modulator Symposium, June 1984 [Los Alamos Report no. LA-UR-84-1921 (unpublished)].
[41]D. W. MacArthur, K. B. Butterfield, D. A. Clark, J. B. Donahue, P. A. M. Gram, H. C. Bryant, C. J. Harvey, and G. Comtet, Phys. Rev. A **32**, 1921 (1985).
[42]U. Fano and J. W. Cooper, Phys. Rev. **137**, A1364 (1965); *ibid.* **138**, A400 (1965).
[43]G. Breit and E. Wigner, Phys. Rev. **49**, 519 (1936).
[44]W. E. Wentworth, J. Chem. Ed. **42**, 96 (1965).
[45]W. E. Demming, *Statistical Adjustment of Data* (Wiley, New York, 1943).
[46]Stanley Cohen, Ph.D. dissertation University of New Mexico [LANL Report No. LA-10726-T, 1986 (unpublished)].
[47]J. A. Simpson, M. G. Menendez, and S. R. Mielczarek, Phys. Rev. **150**, 76 (1964).
[48]G. Comtet, C. J. Harvey, J. E. Stewart, H. C. Bryant, K. B. Butterfield, D. A. Clark, J. B. Donahue, P. A. M. Gram, D. W. MacArthur, V. Yuan, W. W. Smith, and Stanely Cohen, Phys. Rev. A **35**, 1547 (1987).
[49]Particle Data Group, Phys. Lett. **111B**, 17 (1982).
[50]H. A. Bethe and E. E. Salpeter, *Quantum Mechanics of One and Two Electron Atoms* (Springer-Verlag, Berlin, 1957), pp. 232–234.
[51]P. G. Burke, S. Ormonde, and W. Wittaker, Proc. Phys. Soc. London **92**, 319 (1967).
[52]R. S. Oberoi, J. Phys. B **5**, 1120 (1972).
[53]K. T. Chung, Phys. Rev. A **6**, 1809 (1972).
[54]D. R. Herrick and O. Sinanoglu, Phys. Rev. A **11**, 97 (1975).
[55]L. A. Morgan, M. R. C. McDowell, and J. Callaway, J. Phys. B **10**, 3297 (1977).
[56]Y. K. Ho, J. Phys. B **10**, L373 (1977).
[57]L. Lipsky, R. Anania, and M. J. Coonleey, At. Data Nucl. Data Tables **20**, 127 (1977).
[58]J. Callaway, Phys Lett. **75A**, 43 (1979).
[59]C. H. Greene, J. Phys. B **13**, L39 (1980).